DALTON
FULL PAPER

C_2-Symmetric ligands containing hydrogen bond donors: synthesis and properties of Cu(II) complexes of 2,6-bis[*N,N′*-(2-carboxamidophenyl)carbamoyl]pyridine

Zahida Shirin,[a] Joel Thompson,[a] Louise Liable-Sands,[b] Glenn P. A. Yap,[b] Arnold L. Rheingold[b] and A. S. Borovik *[a]

[a] *Department of Chemistry, University of Kansas, Lawrence, Kansas, 66045, USA*
[b] *Department of Chemistry, University of Delaware, Newark, Delaware, 19716, USA*

Received 7th August 2001, Accepted 25th February 2002
First published as an Advance Article on the web 21st March 2002

The synthesis of the new tridentate ligands 2,6-bis[*N,N′*-(2-acetamidophenyl)carbamoyl]pyridine ($H_4\mathbf{1}^{Me}$) and 2,6-bis[*N,N′*-(2-ferrocenylamidophenyl)carbamoyl]pyridine ($H_4\mathbf{1}^{Fc}$), and their corresponding Cu^{II} complexes is described. In the crystalline phase, $H_4\mathbf{1}^{Fc}$ has a helical structure, which is maintained by a network of intramolecular hydrogen bonds. X-Ray diffraction studies on $[CuH_2\mathbf{1}^{Me}(OAc)\cdot Cl]^{2-}$, $[CuH_2\mathbf{1}^{Me}(Cl)\cdot Cl]^{2-}$, and $[CuH_2\mathbf{1}^{Fc}(OAc)\cdot Cl]^{2-}$ reveal that the $[H_2\mathbf{1}^{R}]^{2-}$ ligands bind meridionally. One additional ligand (either OAc^- or Cl^-) binds *trans* to the pyridyl nitrogen to complete coordination in the equatorial plane. The remaining chloride ion (Cl(1)) binds to a second sphere-binding site, which is formed by two convergent hydrogen bonding amide groups. Long Cu ⋯ Cl(1) bonds distances of >2.75 Å are observed. Electrochemical measurements show a 65 mV cathodic shift in the half-wave potential for $[CuH_2\mathbf{1}^{Fc}(OAc)\cdot Cl]^{2-}$ compared to the free ligand $H_4\mathbf{1}^{Fc}$.

Introduction

A variety of biochemical and synthetic systems utilize the secondary coordination spheres around a metal ion to direct or enhance chemistry. This is exemplified by the active sites in metalloproteins.[1] Placement of amino acid residues near a metal center(s) can control key properties such as polarity, electrostatics and solvation. In addition, the structure of the metal active sites can govern the accessibility of exogenous ligands or substrates, influencing selectivity and product formation.[1,2] Hydrogen bonding groups are often used for this purpose, where the H-bonds orient incoming groups or stabilize metal–ligand adducts.

Similar types of approaches have been designed into synthetic systems. The most common method places sterically bulky groups around vacant coordination sites on the metal ion. Tris(pyrazolyl)borates,[3] triazacyclononanes,[4] tris(alkylsilylamido)amines,[5] oxazolines,[6] and Jacobsen's chiral salens[7] are examples of systems that regulate access to a metal ion by appending bulky substituents from synthetic ligands. Hydrogen bond (H-bond) groups have also been incorporated into multidentate ligands.[8] Most of these systems function by having external ligands bind to the metal center with concurrent H-bonding to the multidentate ligands.

In previous reports we have shown that double deprotonation of compounds with 2,6-bis(carbamoyl)pyridyl units affords meridional chelates, which are planar after coordination to a metal ion.[9] Aryl groups have frequently been appended from the amidate nitrogens and used to create rigid organic frameworks around vacant coordination sites on the metal ion. These frameworks affect the overall structural properties of the complexes. For example, helical complexes of $[H_2\mathbf{1}^{Hel}]^{2-}$ have been isolated because the appended H-bonded arrays orient above and below the chelate plane. The complexes were used to examine the assembly of helical arrays in crystal lattices.[9a,b]

We have found that binding a fourth ligand occurs within the equatorial plane, *trans* to the pyridyl nitrogen, which causes the aryl rings to orient nearly perpendicular to the metal–bis(carbamoyl)pyridyl plane. This arrangement of appended aryl groups provides a convenient framework for introducing additional functionality that can assist in binding other ligands. In particular, carboxyamide groups at the *ortho* positions on the phenyl rings will place H-bond donors near, but not coordinated to, the chelated metal ion. These H-bond donors can interact with additional ligands that would bind to the axial coordination sites on the metal ion.

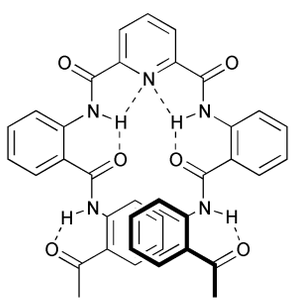

$H_4\mathbf{1}^{Hel}$

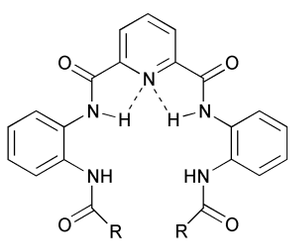

R = Me, $H_4\mathbf{1}^{Me}$
R = Ferrocenyl, $H_4\mathbf{1}^{Fc}$

To explore this design concept, we have made the ligands $H_4\mathbf{1}^{Me}$ and $H_4\mathbf{1}^{Fc}$, and their corresponding Cu^{II} complexes. Solid state structural studies of $[CuH_2\mathbf{1}^{Me}(X)\cdot Cl]^{2-}$ ($X = Cl^-$, OAc^-) demonstrate that both carboxyamide groups intramolecularly H-bond to a single chloride ion. Furthermore, anion binding can be observed electrochemically in $[CuH_2\mathbf{1}^{Fc}(OAc)\cdot Cl]^{2-}$, where shifts in the $E_{1/2}$ values of the appended ferrocenes are observed.

Experimental

All reagents and solvents were purchased from commercial sources and used as received, unless noted otherwise. The syntheses of all metal complexes were conducted in a Vacuum Atmosphere drybox under an argon atmosphere. Elemental analyses of all compounds were performed at Desert Analytics, Tucson, AZ. All samples were dried *in vacuo* before analysis. FT-IR and ^1H NMR spectroscopy were used to corroborate the presence of solvates.

 DOI: 10.1039/b107166c

Syntheses

[*N*-(2-Aminophenyl)amino]acetamide (2). Acetic anhydride (0.94 g, 9.2 mmol) was added dropwise to a solution of phenylenediamine (1.0 g, 9.2 mmol) dissolved in 20 mL of dry CH_2Cl_2 at 0 °C. The reaction mixture was stirred for 2 h at 0 °C during which time a white precipitate formed. The reaction mixture was refrigerated overnight, resulting in the formation of a white crystalline compound that was collected by filtration. The compound was washed with cold CH_2Cl_2, Et_2O and dried under vacuum to yield **2**, as a white solid (0.75 g, 54%). δ_H(400 MHz; solvent DMSO-d_6 standard $SiMe_4$) 9.09 (1 H, s, NH), 7.15 (1 H, d, *J* 7.8 Hz, ArH), 6.88 (1 H, dd, *J* 7.8 Hz, 7.8 Hz, ArH), 6.70 (1 H, d, *J* 7.8 Hz, ArH), 6.52 (1 H, dd, *J* 7.8 Hz, 7.8 Hz, ArH), 4.83 (2 H, s, NH_2), 2.02 (3 H, s, CH_3). δ_C(400 MHz; solvent DMSO-d_6 standard $SiMe_4$) 169.05 (CO); 142.81, 126.59, 126.19, 124.36, 116.94, 116.63 (Ar); 24.16 (Me). FT-IR/cm^{-1} (Nujol) $\tilde{\nu}$ 3455m, 3362m, 3260m (NH_2); 1641s, 1587s, 1535s, 1497s (CO, NH, and aromatic C=C). *m*/*z* 150 (M^+). mp 130–134 °C.

***N*-(2-Aminophenyl)aminocarbonyl]ferrocene (3).** Oxalyl chloride (1.17 g, 9.22 mmol) was pipetted into a 25 mL solution of dry CH_2Cl_2 containing ferrocenemonocarboxylic acid (2.12 g, 9.22 mmol) and one drop of DMF. The reaction was allowed to stir in the dark for 5 h at 0 °C under N_2. Volatiles were removed under reduced pressure, and the solid was triturated with petroleum ether (bp 35–60 °C). Ferrocenecarbonyl chloride (2.04 g) was isolated after removal of solvent under reduced pressure and was used without further isolation. A THF solution of ferrocenecarbonyl chloride (2.04 g) was then added dropwise to a THF solution of 1,2-phenylenediamine (0.887 g, 8.21 mmol) and triethylamine (0.831 g, 8.21 mmol) at −50 °C. The reaction was monitored by TLC (4 : 1 $CHCl_3$: EtOAc) using the disappearance of the 1,2-phenylenediamine spot to indicate completion of the reaction. The reaction mixture was then filtered to remove the triethylammonium hydrochloride salt and the filtrate dried under reduced pressure. The resulting yellow–orange solid was dissolved in chloroform, washed with water and extracted with 1 M HCl. The product was isolated by precipitation by adjusting the pH > 12 with 1 M NaOH. The resulting yellow solid was collected on a medium glass frit, rinsed with H_2O, and dried at 100 °C under reduced pressure to give **3** (1.25 g, 49%). δ_H(400 MHz; solvent DMSO-d_6 standard $SiMe_4$) 9.16 (1 H, s, NH), 7.08 (1 H, d, *J* 7.8 Hz, ArH), 6.98 (1 H, dd, *J* 7.8 Hz, 7.8 Hz, ArH), 6.80 (1 H, d, *J* 7.8 Hz, ArH), 6.63 (1 H, dd, *J* 7.8 Hz, 7.8 Hz, ArH), 4.97 (2 H, m, Fc), 4.81 (2 H, s, NH_2), 4.43 (2 H, m, Fc), 4.24 (5 H, s, Fc). δ_C(400 MHz; solvent DMSO-d_6 standard $SiMe_4$) 167.99 (CO), 143.12, 126.63, 126.29, 123.83, 116.63, 116.50 (Ar), 76.15, 70.38, 69.56, 68.67 (Fc). FT-IR/cm^{-1} (Nujol), $\tilde{\nu}$ 3476m, 3384m (NH_2); 3271s (NH); 1636s (CO). mp 190 °C (decomp.). *m*/*z* 319.2 (FAB^-, NBA + CH_2Cl_2 matrix).

2,6-Bis[*N*,*N*′-(2-acetamidophenyl)carbamoyl]pyridine ($H_4\mathbf{1}^{Me}$). Triethylamine (1.05 mL, 7.50 mmol) was added into a solution of **2** (1.0 g, 6.7 mmol) in 50 mL of dry THF at −50 °C under dinitrogen. Pyridine-2,6-dicarbonyl dichloride (0.77 g, 3.8 mmol) was dissolved in 5.0 mL of THF and added dropwise to the above mixture. The reaction was monitored using TLC by the disappearance of the monoacylated starting reagent. Triethylamine hydrochloride was removed by filtration after 2 h stirring and volatiles removed under reduced pressure. The residue was dissolved in chloroform, washed with water, 5% NaOH, brine, and anhydrous Na_2SO_4. Volatiles were removed under reduced pressure and the residue was washed with diethyl ether to yield a white solid $H_4\mathbf{1}^{Me}$ (1.25 g, 77%). δ_H(400 MHz; solvent DMSO-d_6 standard $SiMe_4$) 10.93 (2 H, s, NH), 9.77 (2 H, s, NH), 8.39 (2 H, m, pyH), 8.32 (1 H, m, pyH), 7.75 (2 H, m, ArH), 7.56 (2 H, m, ArH), 7.25 (4 H, m, ArH), 1.91 (6 H, s, CH_3). δ_C(400 MHz; solvent DMSO-d_6 standard $SiMe_4$) 170.34, 162.46 (CO); 149.43, 141.06, 132.51, 130.52, 126.61, 126.45, 125.89, 125.33 (Ar), 24.15 (Me) (observed 11 out of 12 expected signals). FT-IR/cm^{-1} (Nujol) $\tilde{\nu}$ 3278m, 3240m, 3285m, 3128m (NH); 1683s, 1664s, 1645s (CO). mp 270–274 °C. *m*/*z* 432.2 (FAB^+, TG/G + DMSO matrix).

2,6-Bis[*N*,*N*′-(2-ferrocenylamidophenyl)carbamoyl]pyridine ($H_4\mathbf{1}^{Fc}$). $H_4\mathbf{1}^{Fc}$ was synthesized by a similar procedure to that used for $H_4\mathbf{1}^{Me}$ using **3** (1.8 g, 5.7 mmol). The yellow–orange $H_4\mathbf{1}^{Fc}$ was isolated in 70% yield (1.6 g). δ_H(500 MHz; solvent DMSO-d_6 standard $SiMe_4$), 11.3 (2 H, s, NH), 9.69 (2 H, s, NH), 8.50 (2 H, d, *J* 7.8 Hz, pyrH), 8.38 (1 H, t, *J* 7.8 Hz, pyrH), 8.00 (2 H, d, *J* 7.8 Hz ArH), 7.62 (2 H, d, *J* 7.8 Hz, ArH), 7.45 (2 H, dd, *J* 7.8 Hz, 7.8 Hz, ArH), 7.39 (2 H, dd, *J* 7.8 Hz, 7.8 Hz, ArH), 4.68 (4 H, FcH), 4.21 (4 H, FcH), 3.94 (10 H, FcH). δ_C(500 MHz; solvent DMSO-d_6 standard $SiMe_4$) 169.57, 161.13 (CO); 148.04, 141.12, 130.76, 130.29, 126.52, 126.06, 125.78, 125.47, 124.65 (Ar); 74.62, 70.94, 69.35, 68.39 (Fc). FT-IR/cm^{-1} (Nujol) $\tilde{\nu}$ 1695s, 1599s, 1526s (CO). *m*/*z* 771.2 (FAB^+, NBA + CH_3CN matrix). $E_{1/2}$ = 340 mV (*vs.* $Ag^{+/0}$, ΔE_p = 111 mV, $i_a \times i_c^{-1}$ = 1.07, CH_3CN).

$(Et_4N)_2[CuH_2\mathbf{1}^{Me}(OAc)\cdot Cl]$. $H_4\mathbf{1}^{Me}$ (0.20 g, 0.46 mmol) was dissolved in DMF and treated with solid KH (0.037 g, 0.92 mmol). After the gas evolution ceased, solid $Cu(OAc)_2$ (0.084 g, 0.46 mmol) was added, which caused a color change from yellow to green. The mixture was stirred for 2 h after which 1 equivalent of KOAc was separated by filtration. Two equivalents of Et_4NCl (0.15 g, 0.92 mol) were then added to the filtrate and the mixture was allowed to stir for 2 h. The insoluble product (KCl) was separated by filtration and the filtrate was concentrated under reduced pressure to yield a green solid, which was dissolved in CH_3CN and kept for crystallization by slow diffusion of diethyl ether (0.320 g, 78%). Found: C, 58.12; H, 7.47; N, 12.71. $(Et_4N)_2[CuH_2\mathbf{1}^{Me}(OAc)\cdot Cl]\cdot CH_3CN$ ($C_{43}H_{65}Cl\,CuN_8O_6$) requires C, 58.09; H, 7.37; N, 12.60%. FT-IR/cm^{-1} (Nujol) $\tilde{\nu}$ 3212m, 3165m (NH); 1669s, 1625s, 1607s, 1588s (CO). λ_{max}/nm (CH_3CN) 620 (ε/mol dm^{-3} cm^{-1} 230). μ_{eff} = 1.92 μ_B (solid, 298 K). $g_\parallel$ = 2.22, $A_\parallel$ = 178 G, $g_\perp$ = 2.04, $A_\perp$ = 14 G (CH_2Cl_2/toluene, 77 K).

$(Et_4N)_2[CuH_2\mathbf{1}^{Me}(Cl)\cdot Cl]$. This compound was synthesized following the route used for $(Et_4N)_2[CuH_2\mathbf{1}^{Me}(OAc)(Cl)]$ using $CuCl_2$ (0.062 g, 0.46 mmol) as the metal ion precursor. The salt was isolated as a green crystalline solid in 80% yield (0.30 g). Found: C, 56.53; H, 7.05; N, 11.74. $(Et_4N)_2[CuH_2\mathbf{1}^{Me}(Cl)\cdot Cl]$ ($C_{39}H_{59}Cl_2CuN_7O_4$) requires C, 56.82; H, 7.21; N, 11.89%. FT-IR/cm^{-1} (Nujol) $\tilde{\nu}$ 3205m, 3164m (NH); 1668s, 1627s, 1607s, 1587s (CO). λ_{max}/nm (CH_3CN) 634 (ε/mol dm^{-3} cm^{-1} 338). μ_{eff} = 1.90 μ_B (solid, 298K), $g_\parallel$ = 2.21, $A_\parallel$ = 175 G, $g_\perp$ = 2.04 (CH_2Cl_2/toluene, 77 K).

$(Et_4N)_2[CuH_2\mathbf{1}^{Fc}(OAc)\cdot Cl]$. This compound was synthesized by the same route as $(Et_4N)_2[Cu(H_2\mathbf{1}^{Me})(OAc)(Cl)]$ using $H_4\mathbf{1}^{Fc}$ (0.355 g, 0.46 mmol) and $Cu(OAc)_2$ (0.84 g, 0.46 mmol). The compound was purified by crystallization with CH_3CN and diethyl ether, to yield green crystals (0.320 g, 59% yield). Found: C, 58.76; H, 6.35; N, 8.13. $(Et_4N)_2[CuH_2\mathbf{1}^{Fc}(OAc)\cdot Cl]\cdot CH_3CN$ ($C_{59}H_{76}ClCuFe_2N_7O_7$) requires C, 58.76; H, 6.35; N, 8.12%. FT-IR/cm^{-1} (Nujol) $\tilde{\nu}$ 3212m, 3165m (NH); 1669s, 1625s, 1607s, (CO). λ_{max}/nm (CH_3CN) 603 (ε/mol dm^{-3} cm^{-1} 230). μ_{eff} = 1.92 μ_B (solid, 298K), $g_\parallel$ = 2.22, $A_\parallel$ = 174 G, $g_\perp$ = 2.04, $A_\perp$ = 15 G (DMF, 77 K). $E_{1/2}$ = 275 mV (*vs.* $Ag^{+/0}$, ΔE_p = 95 mV, $i_a \times i_c^{-1}$ = 1.19, CH_3CN).

$K[CuH_2\mathbf{1}^{Fc}(OAc)]$. $H_4\mathbf{1}^{Fc}$ (0.26 g, 0.34 mmol) in DMF was deprotonated with KH (0.027 g, 0.68 mmol) under an argon atmosphere. The reaction was allowed to continue until H_2 evolution ceased. Solid $Cu(OAc)_2$ (0.061 g, 0.34 mmol) was

Table 1 Crystallographic data for $H_4\mathbf{1}^{Fc}\cdot 0.25CH_2Cl_2$, $(Et_4N)_2[CuH_2\mathbf{1}^{Me}(OAc)\cdot Cl]\cdot 1.5CH_3CN$, and $(Et_4N)_2[CuH_2\mathbf{1}^{Me}(Cl)\cdot Cl]\cdot CH_3CN$

Complex	$H_4\mathbf{1}^{Fc}\cdot 0.25CH_2Cl_2$	$(Et_4N)_2[CuH_2\mathbf{1}^{Me}(OAc)\cdot Cl]\cdot 1.5CH_3CN$	$(Et_4N)_2[CuH_2\mathbf{1}^{Me}(Cl)\cdot Cl]\cdot CH_3CN$
Empirical formula	$C_{41.25}H_{34.50}Cl_{0.50}Fe_2N_5O_4$	$C_{44}H_{66.5}ClCuN_{8.50}O_6$	$C_{41}H_{62}Cl_2CuN_8O_4$
M	793.66	909.55	865.43
T/K	298(2)	213(2)	100(2)
Crystal system	Triclinic	Orthorhombic	Triclinic
Space group	$P\bar{1}$	$Pna2_1$	$P\bar{1}$
a/Å	9.550(2)	29.4699(2)	10.1771(15)
b/Å	12.011(1)	10.1365(2)	14.554(2)
c/Å	16.472(2)	33.1137(3)	15.614(2)
α/°	75.037(9)	90.00	78.999(3)
β/°	87.880(8)	90.00	76.045(3)
γ/°	79.788(13)	90.00	74.908(3)
Z	2	8	2
V/Å^3	1796(1)	9891.8(2)	2146.7(5)
μ_{calc}/mm^{-1}	0.895	0.547	0.683
ρ_{calc}/g cm^{-3}	1.467	1.221	1.339
F (000)	819	3872	918
Crystal dimensions/mm	0.40 × 0.20 × 0.10	0.02 × 0.4 × 0.4	0.28 × 0.17 × 0.12
Radiation	Mo-Kα (λ = 0.71073 Å)	Mo-Kα (λ = 0.71073 Å)	Mo-Kα (λ = 0.71073 Å)
Reflections collected	5630	29695	18416
Independent reflections	4630 (R_{int} = 0.0296)	15010 (R_{int} = 0.0480)	12393 (R_{int} = 0.0273)
R^a	0.0577	0.0548	0.0661
$R_w{}^b$	0.1654	0.1144	0.2012
GOF ^{c}	1.031	1.303	1.036

^{a} $R = [\Sigma|\Delta F|/\Sigma|F_o|]$. ^{b} $R_w = [\Sigma w(\Delta F)^2/\Sigma wF_o^2]$. ^{c} Goodness of fit on F^2.

added in one portion and the solution changed in color from brown to olive green. The insoluble product (KOAc, 1 equivalent) was removed by filtration. The filtrate was concentrated to dryness under reduced pressure to yield 0.323 g of crude $K[Cu(H_2\mathbf{1}^{Fc})(OAc)]$, which was purified by vapor diffusion of Et_2O into a concentrated CH_3CN solution of the complex under ambient conditions. Found: C, 53.1; H, 4.18; N, 7.75. $K[Cu(H_2\mathbf{1}^{Fc})(OAc)]\cdot 2H_2O$ ($C_{43}H_{38}Cu\ Fe_2KN_5O_8$) requires C, 53.4; H, 3.96; N, 7.24%. FT-IR/cm^{-1} (KBr) $\tilde{\nu}$ 3274, 3081 (NH); (Nujol) 1669, 1652 (CO); 1611, 1514, 759; 1585 (NH); 1307 (CN). λ_{max}/nm (CH_3CN) 585sh. $E_{1/2}$ = 310 mV (*vs.* $Ag^{+/0}$, ΔE = 110 mV, $i_a \times i_c^{-1}$ = 1.08, CH_3CN).

Physical methods

Fast atom bombardment mass spectra (FAB-MS) were recorded on a Hewlett-Packard 5989 A spectrometer with a HPLC (HP 1050) HP particle-beam interface mass system and a phasor FAB gun. FAB experiments were carried out in either a nitrobenzyl alcohol (NBA) or thioglycerol/glycerol (TG/G) matrix and a xenon fast atom beam was used. Fourier transform infrared spectra were recorded on an ATI Mattson Genesis Series FTIR spectrometer, and are reported in wavenumbers. Solid samples were pressed in a KBr matrix or prepared in mineral oil and run between KBr plates. ^{1}H and ^{13}C NMR spectra were recorded on a Bruker 400 MHz spectrometer. Chemical shifts are reported in ppm relative to the internal standard $SiMe_4$. Electron paramagnetic resonance spectra were collected using a Bruker EMX spectrometer equipped with an ER4102ST cavity. The instrument was previously calibrated using DPPH. Spectrometer settings: microwave frequency, 9.296 GHz; microwave power, 0.635 mW; modulation frequency, 100 kHz and modulation amplitude, 5.02 G. Solid state magnetic moments were determined using a Johnson Matthey magnetic susceptibility balance calibrated with mercury(II) tetrathiocyanatocobaltate(II) (χ_γ = 16.44(10^{-6}) ± 0.08 cm^3 g^{-1}).[10] Electrochemical data were obtained using a BAS CV 50W. Experiments were performed in a three-electrode cell consisting of a glassy carbon working electrode, Pt wire auxiliary electrode and Ag/Ag^+ reference electrode equipped with a Vycor tip. A ferrocenium/ferrocene couple was used to monitor the reference electrode and was observed at 94 mV with $i_a \times i_c^{-1}$ = 1.00 and ΔE_p = 72 mV. Cyclic voltammograms were collected at a scan rate of 0.500 V s^{-1} in acetonitrile containing 0.1 M tetrabutylammonium hexafluorophosphate. Electronic spectra were collected on a Cary 50 spectrophotometer using 1.00 cm Suprasil quartz cuvets.

Crystallographic structural determination

Crystal data collection, and refinement parameters for $[H_4\mathbf{1}^{Fc}]\cdot 0.25CH_2Cl_2$, $(Et_4N)_2[CuH_2\mathbf{1}^{Me}(OAc)\cdot Cl]\cdot 1.5CH_3CN$, and $(Et_4N)_2[CuH_2\mathbf{1}^{Me}(Cl)\cdot Cl]$ are given in Table 1. For $[H_4\mathbf{1}^{Fc}]\cdot 0.25CH_2Cl_2$ and $(Et_4N)_2[CuH_2\mathbf{1}^{Me}(Cl)\cdot Cl]$ no evidence of symmetry higher than triclinic was observed in either photographic or diffraction data. The *E*-statistics suggested a centrosymmetric space group. Solutions in $P\bar{1}$ yielded chemically reasonable and computationally stable results. For $(Et_4N)_2[CuH_2\mathbf{1}^{Me}(OAc)\cdot Cl]\cdot 1.5CH_3CN$, the systematic absences in the data indicated either of the orthorhombic space groups, $Pna2_1$ or *Pnma*. Initially, the noncentrosymmetric alternative was suggested by *E*-statistics, and later verified by the results of refinement. Crystallographic mirror planes are neither aligned within the structures or between them. The structures were solved using direct methods, completed by subsequent difference Fourier syntheses and refined by full-matrix least-squares procedures on F^2. Absorption corrections were not required for $[H_4\mathbf{1}^{Fc}]\cdot 0.25CH_2Cl_2$ and $(Et_4N)_2[CuH_2\mathbf{1}^{Me}(Cl)\cdot Cl]$ because of <10% variation in the ψ-scans. All non-hydrogen atoms were refined with anisotropic displacement parameters. Hydrogens atoms were treated as idealized contributions. The asymmetric unit of $(Et_4N)_2[CuH_2\mathbf{1}^{Me}(OAc)\cdot Cl]\cdot 1.5CH_3CN$ consists of two independent Cu complexes, four Et_4N^+ counter ions, and three molecules of acetonitrile. All software and sources of the scattering factors are contained in the SHELXTL (5.3) program library (G. Sheldrick, Siemens XRD, Madison, WI).

CCDC reference numbers 168574–168576.

See http://www.rsc.org/suppdata/dt/b1/b107166c/ for crystallographic data in CIF or other electronic format.

Results and discussion

Design consideration

Our initial ligands had the carbonyl groups of the amides attached at *ortho*-positions of the appended phenyl rings, as in $H_4\mathbf{1}^{Hel}$. This placement allowed the carbonyl oxygens to interact

with the metal ion bonded to the bis(carbamoyl)pyridyl unit. This coordination was promoted by the formation of six-membered chelate rings. The current ligands, $H_4\mathbf{1}^{Me}$ and $H_4\mathbf{1}^{Fc}$, are derivatives of these early systems, with the appended groups having the NH portion of the amide bonded to the phenyl rings. These ligands do not have the correct geometric features to directly bind to the metal center. However, the NH groups can H-bond to exogenous ions or molecules. Fig. 1 illustrates

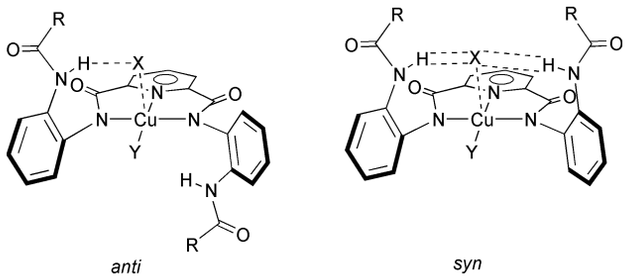

Fig. 1 The *anti* and *syn* conformations of the appended arms in $[MH_2\mathbf{1}^{R}(Y)\cdot X]^{n+}$ showing the H-bonding interactions.

the two conformations that are possible. The *anti* conformation places the appended NH groups on opposite faces of the bis(carbamoyl)pyridyl chelate plane. One H-bond can occur between the appended amide and an external species. In contrast, the *syn* conformation positions both appended amides on one side of the chelate plane. This conformation creates a binding pocket around one of the axial coordination sites on the metal, resulting in two H-bond interactions with an incoming ligand. Moreover, the amides can be equipped with redox-active R groups, such as in $H_4\mathbf{1}^{Fc}$, to monitor external ligand binding.

Synthesis

The synthetic routes for the ligands and complexes are outlined in Scheme 1. The synthesis of $H_4\mathbf{1}^{Me}$ and $H_4\mathbf{1}^{Fc}$ began with

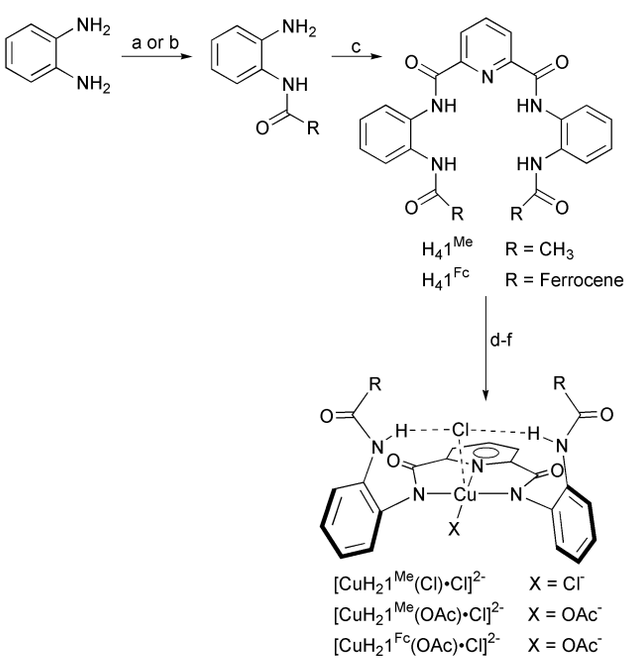

Scheme 1 Conditions: (a) acetic anhydride, 0 °C, CH_2Cl_2, N_2; (b) ferrocene monocarbonyl chloride, Et_3N, −50 °C, THF; (c) pyridine dicarbonyl dichloride, Et_3N, −50 °C, THF; (d) KH, DMF, Ar; (e) $Cu(OAc)_2$ or $CuCl_2$; (f) Et_4NCl.

monoacylating of 1,2-phenylenediamine with either acetic anhydride or ferrocenecarbonyl chloride. Yields of *ca.* 50% were obtained for this step. These yields are relatively low because diacylated products were also produced. Controlling the reaction temperature and dropwise addition of the acylating agents were used to minimize the diacyl products. Separation of the mono- and di-amides was accomplished by sequential acid/base extractions. Treating the monoacylated compounds with pyridinedicarbonyl dichloride resulted in $H_4\mathbf{1}^{Me}$ and $H_4\mathbf{1}^{Fc}$ in overall isolated yields of 42% and 34%.

The metal complexes were made by deprotonating the pyridyl amides of $H_4\mathbf{1}^{Me}$ and $H_4\mathbf{1}^{Fc}$ with 2 equivalents of KH. Without isolation, $[H_2\mathbf{1}^{Me}]^{2-}$ and $[H_2\mathbf{1}^{Fc}]^{2-}$ were treated with the appropriate Cu^{II} salts. $K[CuH_2\mathbf{1}^{Fc}(OAc)]$ was isolated by this method in 50% yield. In most cases, the complexes were metathesized with 2 equivalents of Et_4NCl, which produced the dianionic complexes $[CuH_2\mathbf{1}^{Me}(OAc)\cdot Cl]^{2-}$, $[CuH_2\mathbf{1}^{Me}(Cl)\cdot Cl]^{2-}$, and $[CuH_2\mathbf{1}^{Fc}(OAc)\cdot Cl]^{2-}$. Note that the second equivalent of chloride ion for the metathesis salt precipitated from the reaction mixture as KCl. Isolated yields for the tetraethylammonium salts of the complexes range from 60–80%. The complexes are hydroscopic if stored in the open, yet are stable for months in the solid state under an inert atmosphere.

Molecular structure results

Single crystal diffraction studies were done on $H_4\mathbf{1}^{Fc}\cdot 0.25CH_2Cl_2$, $(Et_4N)_2[CuH_2\mathbf{1}^{Me}(OAc)\cdot Cl]\cdot 1.5CH_3CN$, and $(Et_4N)_2[CuH_2\mathbf{1}^{Me}(Cl)\cdot Cl]$. Selected bond distances and angles for the two metal salts are given in Table 2. For $(Et_4N)_2[CuH_2\mathbf{1}^{Me}(OAc)\cdot Cl]$ two independent, but essentially identical, anions were found in the asymmetric unit. These are denoted $[CuH_2\mathbf{1a}^{Me}(OAc)\cdot Cl]^{2-}$ and $[CuH_2\mathbf{1b}^{Me}(OAc)\cdot Cl]^{2-}$.

Fig. 2 shows a view of the molecular structure of $H_4\mathbf{1}^{Fc}$. In

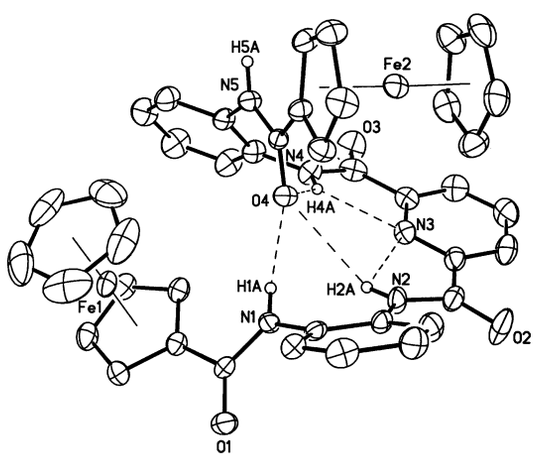

Fig. 2 Thermal ellipsoid diagram of $H_4\mathbf{1}^{Fc}$ showing the intramolecular H-bond network. The ellipsoids are drawn at the 40% probability level and only the amide hydrogens are shown for clarity.

the solid state the compound is helical. The molecule has an intramolecular network of H-bonds, which assists in maintaining helicity. Bifurcated H-bonds are observed between the pyridyl nitrogen N(3), the carbamoyl hydrogens H(2A) and H(4A), and amide carbonyl oxygen O(4) that connects one of the ferrocene groups to an aryl ring. The relevant heavy atom distances for these interactions are: N(3) ··· N(2) = 2.689, N(3) ··· N(4) = 2.658, N(2) ··· O(4) = 3.266, and N(4) ··· O(4) = 2.718 Å. There is an additional H-bond between the amide group containing N(1) and O(4) (N(1) ··· O(4) = 2.803 Å). Taken together, these H-bonds cause the ferrocene group containing Fe(2) to be twisted in the direction of the pyridyl ring, producing the observed helical structure. The molecular structure of $H_4\mathbf{1}^{Fc}$ is reminiscent of that found in the solid state for the optically pure compounds, 2,6-bis[{2-L-methylglycinyl)carbamoylphenyl}carbamoyl]pyridine (**4**).[9d] Molecular helices are also found in the

Table 2 Selected bond distances (Å) and angles (°) for $[CuH_2\mathbf{1}^{Me}(Cl)\cdot(Cl)]^{2-}$ and $[CuH_2\mathbf{1}^{Me}(OAc)\cdot(Cl)]^{2-}$

	$[CuH_2\mathbf{1}^{Me}(Cl)\cdot(Cl)]^{2-}$	$[CuH_2\mathbf{1a}^{Me}(OAc)\cdot(Cl)]^{2-}$ ($[CuH_2\mathbf{1b}^{Me}(OAc)\cdot(Cl)]^{2-}$)
Cu–O(5)	na[a]	1.949(3) (1.949(3))
Cu–N(2)	2.038(2)	2.025(4) (2.032(4))
Cu–N(3)	1.944(3)	1.945(4) (1.932(4))
Cu–N(4)	2.037(3)	2.030(5) (2.030(4))
Cu–Cl(1)	2.7483(10)	2.819(4) (2.846(4))
Cu–Cl(2)	2.2564(9)	na
N(1) ··· Cl(1)	3.341(3)	3.216(4) (3.292(4))
N(5) ··· Cl(1)	3.325(3)	3.264(4) (3.268(4))
N(2)–Cu–N(3)	79.23(10)	80.51(18)
N(2)–Cu–N(4)	158.10(11)	160.78(17)
N(3)–Cu–N(4)	79.37(11)	80.29(18)
N(2)–Cu–Cl(2)	99.10(8)	na
N(3)–Cu–Cl(2)	163.84(8)	na
N(4)–Cu–Cl(2)	100.13(8)	na
N(2)–Cu–O(5)	na	100.53(17)
N(3)–Cu–O(5)	na	168.08(16)
N(4)–Cu–O(5)	na	98.10(17)
Cl(1)–Cu–Cl(2)	108.03(3)	na

[a] Not applicable.

structure of **4**, which are maintained by a similar network of intramolecular H-bonds.

Fig. 3 presents the molecular structures for $[CuH_2\mathbf{1}^{Me}(Cl)\cdot$

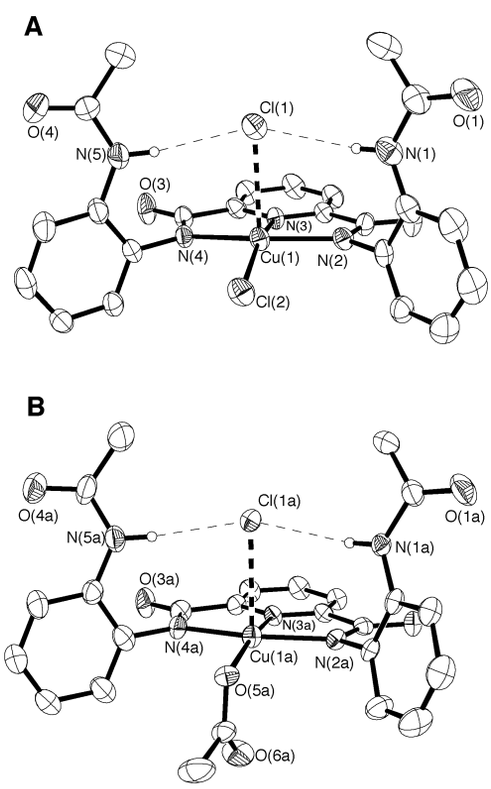

Fig. 3 Thermal ellipsoid diagram of $[CuH_2\mathbf{1}^{Me}(OAc)\cdot Cl]^{2-}$ (**A**) and $[CuH_2\mathbf{1}^{Me}(Cl)\cdot Cl]^{2-}$ (**B**). The ellipsoids are drawn at the 50% probability level and only the amide hydrogens are shown for clarity.

$Cl]^{2-}$ and $[CuH_2\mathbf{1}^{Me}(OAc)\cdot Cl]^{2-}$. Both complexes have four ligands in the equatorial plane, three of which are nitrogen donors from the tridentate bis(carbamoyl)pyridyl unit. In $[CuH_2\mathbf{1}^{Me}(Cl)\cdot Cl]^{2-}$, the fourth ligand is a chloride ion (Cl(2)), which is nearly *trans* to N(3) (N(3)–Cu–Cl(2) = 163.84(8)°). The two Cu–N_{amide} distances are longer than the Cu–N(3) bond, which is expected based on previously reported Cu^{II} complexes with bis(carbamoyl)pyridyl.[9] Similar metrical properties were found for $[CuH_2\mathbf{1}^{Me}(OAc)\cdot Cl]^{2-}$, with the exception that an acetate ion is positioned *trans* to N(3) (Table 2). Note that the acetate ion is monodentate with only O(5) bonded to the copper center (O(6) is >2.8 Å from Cu(1)).

The binding of Cl(2) and acetate in $[CuH_2\mathbf{1}^{Me}(Cl)\cdot Cl]^{2-}$ and $[CuH_2\mathbf{1}^{Me}(OAc)\cdot Cl]^{2-}$ causes the appended aryl rings to be positioned nearly perpendicular to the coordination plane. In $[CuH_2\mathbf{1}^{Me}(Cl)\cdot Cl]^{2-}$ dihedral angles of 94.0 and 90.8° are found between the coordination plane and the planes formed by the aryl rings. In addition, the dihedral angle between the aryl groups is 82.3°. For $[CuH_2\mathbf{1}^{Me}(OAc)\cdot Cl]^{2-}$ the dihedral angles between the coordination plane and aryl planes are 101.2 and 94.5° for anion **a** and 108.4 and 98.0° for anion **b**. The planes of the aryl rings are also nearly perpendicular to each other: dihedral angles between aryl planes of 84.5 and 83.1° are found for anions **a** and **b**, respectively. This disposition of appended aryl group induces an L-shaped cleft around the fourth coordinate site in the basal plane (*i.e.*, *trans* to N(3)). The aryl rings flank two sides of the external ligand: distances of ≈4.0 Å are observed from the centroid of the aryl rings to the coordinated Cl or O atoms.

The most striking feature in the molecular structures of $[CuH_2\mathbf{1}^{Me}(Cl)\cdot Cl]^{2-}$ and $[CuH_2\mathbf{1}^{Me}(OAc)\cdot Cl]^{2-}$ is the conformation adopted by the appended amide groups. The complexes have the appended groups in the *syn* conformations, which positions the amide groups on the same face of the complexes. This conformation produces a second site for external ligands because of the two convergent H-bonding amide groups. In $[CuH_2\mathbf{1}^{Me}(Cl)\cdot Cl]^{2-}$ and $[CuH_2\mathbf{1}^{Me}(OAc)\cdot Cl]^{2-}$, this site is taken by Cl(1), which is H-bonded to the two amide NH groups. The observed N(1) ··· Cl(1) and N(5) ··· Cl(1) distance are <3.4 Å with N–H–Cl(1) angles >150°, which are consistent with the intramolecular H-bond assignment.[11] The binding of Cl(1) in the secondary site places the ion near the Cu^{II} center. The Cu ··· Cl(1) distances range from 2.7483(10) Å in $[CuH_2\mathbf{1}^{Me}(Cl)\cdot Cl]^{2-}$ to 2.846(4) Å in $[CuH_2\mathbf{1b}^{Me}(OAc)\cdot Cl]^{2-}$. These distances are significantly longer than the 2.2–2.4 Å bond lengths that are normally observed for Cu–Cl interactions[12] (see for example, the Cu(1)–Cl(2) distance in $[CuH_2\mathbf{1}^{Me}(Cl)\cdot Cl]^{2-}$). The long Cu ··· Cl(1) distances are comparable to those found for intermolecular Cu ··· Cl interactions in structures of other Cu^{II} salts. Examples where these long bonds are observed include $[MeNH_3]_2[CuCl_4]$[13] and $[C_3H_8N_6][Cu_2Cl_6]$.[14] In the previously reported systems, the long Cu ··· Cl bonds result from the Cu^{II} center in one complex interacting weakly with a chloro ligand on an adjacent complex within a crystal lattice. To our knowledge, these long Cu ··· Cl intermolecular interactions have only been reported in the solid state.

A preliminary X-ray diffraction study on $[CuH_2\mathbf{1}^{Fc}(OAc)\cdot Cl]^{2-}$ shows it has a similar molecular structure to that of $[CuH_2\mathbf{1}^{Me}(OAc)\cdot Cl]^{2-}$ (Fig. 4). The data collected for $(Et_4N)_2[CuH_2\mathbf{1}^{Fc}(OAc)\cdot Cl]$ are not of sufficient quality to obtain detailed metrical information (I/σ number = 2.8, R = 0.014). Nevertheless, it is clear from the present data that in $[CuH_2\mathbf{1}^{Fc}(OAc)\cdot Cl]^{2-}$, the ferrocenyl groups are also in the *syn* conformation, with the chloride ion positioned between the two ferrocenylamide groups.

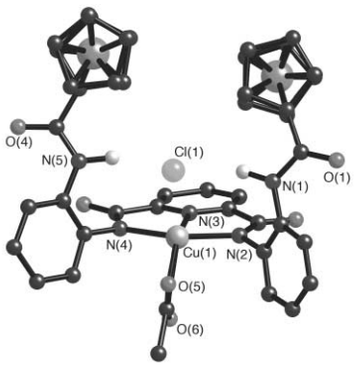

Fig. 4 A ball and stick representation of the preliminary structure for $[CuH_2\mathbf{1}^{Fc}(OAc)\cdot Cl]^{2-}$.

Electrochemistry

The redox potentials of the ferrocenyl groups in $H_4\mathbf{1}^{Fc}$, $[CuH_2\mathbf{1}^{Fc}(OAc)]^-$ and $[CuH_2\mathbf{1}^{Fc}(OAc)\cdot Cl]^{2-}$ were investigated by cyclic voltammetry. Fig. 5 shows their cyclic voltammograms (CV) measured in acetonitrile. The nearly reversible redox couples for each compound are a single wave, which indicates that the two ferrocenyl groups are electrochemically independent. For $H_4\mathbf{1}^{Fc}$, an $E_{1/2}$ = 340 mV *vs.* Ag^+/Ag is found, with ΔE = 110 mV and $i_a \times i_c^{-1}$ = 1.07. The ferrocene half-wave potential in $[CuH_2\mathbf{1}^{Fc}(OAc)]^-$ is at 310 mV *vs.* Ag^+/Ag (ΔE = 110 mV and $i_a \times i_c^{-1}$ = 1.08). This cathodic shift is consistent with the formation of a monoanionic species, which should stabilize the oxidized species.[15] A further cathodic shift of the redox wave is observed in $[CuH_2\mathbf{1}^{Fc}(OAc)\cdot Cl]^{2-}$, which has an $E_{1/2}$ = 275 mV *vs.* Ag^+/Ag, with ΔE = 95 mV and $i_a \times i_c^{-1}$ = 1.19. The −65 mV shift between $H_4\mathbf{1}^{Fc}$ and $[CuH_2\mathbf{1}^{Fc}(OAc)\cdot Cl]^{2-}$ is comparable to shifts found for chloride binding neutral compounds, such as Zn^{II} porphyrins with appended ferrocenes[15] and bis(aminoferrocene) systems.[16–18] Note that the half-wave potential of $H_4\mathbf{1}$ is shifted by only −5 mV when treated with Et_4NCl.

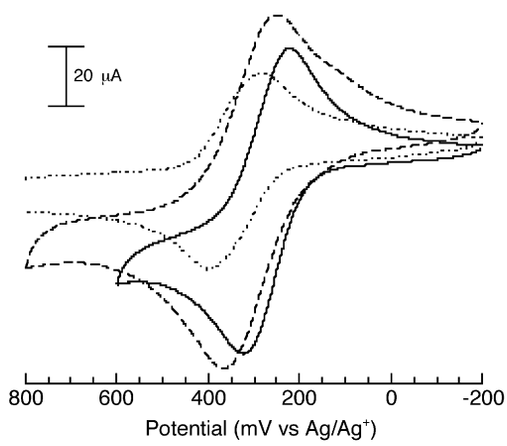

Fig. 5 Cyclic voltammograms of $H_4\mathbf{1}^{Fc}$ (· · ·), $[CuH_2\mathbf{1}^{Fc}(OAc)]^-$ (– – –) and $[CuH_2\mathbf{1}^{Fc}(OAc)\cdot Cl]^{2-}$ (–) recorded in acetonitrile at a scan rate of 500 mV s^{-1}.

Summary

We have described the synthesis of a new series of ligands containing bis(carbamoyl)pyridyl chelates containing appended amide groups that serve as H-bond donors. These ligands have the capability of placing two H-bond donors on the same face of the chelate plane, resulting in the formation of a second sphere-binding site. This concept was demonstrated in the solid state by the molecular structures of $[CuH_2\mathbf{1}^{Me}(OAc)\cdot Cl]^{2-}$, $[CuH_2\mathbf{1}^{Me}(Cl)\cdot Cl]^{2-}$, and the preliminary structure of $[CuH_2\mathbf{1}^{Fc}(OAc)\cdot Cl]^{2-}$. Each structure shows that one chloride ion is H-bonded to the appended amide groups, with only a long (>2.7 Å) interaction with the coordinated Cu^{II} center. Electrochemical studies show that the binding of chloride in $[CuH_2\mathbf{1}^{Fc}(OAc)\cdot Cl]^{2-}$ results in an observable cathodic shift in the half-wave potential of the ferrocenyl groups, when compared to those found in $H_4\mathbf{1}$ and $[CuH_2\mathbf{1}^{Fc}(OAc)]^-$.

Acknowledgements

Acknowledgement is made to the NIH (GM 50781) for financial support.

References

1 (*a*) R. H. Holm, P. Kennepohl and E. I. Solomon, *Chem. Rev.*, 1996, **96**, 2239; (*b*) B. A. Springer, S. G. Sligar, J. S. Olsen and G. N. Philips, Jr., *Chem. Rev.*, 1994, **94**, 699; (*c*) Y. Lu and J. S. Valentine, *Curr. Opin. Struct. Biol.*, 1997, **7**, 495.
2 D. W. Christianson and J. D. Cox, *Annu. Rev. Biochem.*, 1999, **68**, 33.
3 Review W. B. Tolman and N. Kitajima, *Prog. Inorg. Chem.*, 1995, **43**, 419.
4 (*a*) Selected examples: J. L. Sessler, J. W. Sibert and V. Lynch, *Inorg. Chim. Acta*, 1994, **216**, 89; (*b*) J. A. Halfen, S. Mahapatra, E. C. Wilkinson, A. J. Gengenbach, V. G. Young, Jr., L. Que, Jr. and W. B. Tolman, *J. Am. Chem. Soc.*, 1996, **118**, 763; (*c*) W. B. Tolman, *Acc. Chem. Res.*, 1997, **30**, 227 and references therein; (*d*) A. Diehold, A. Elbouadili and K. S. Hagen, *Inorg. Chem.*, 2000, **39**, 3915.
5 (*a*) W. Plass and J. G. Verkade, *J. Am. Chem. Soc.*, 1992, **114**, 2275; (*b*) R. R. Schrock, *Acc. Chem. Res.*, 1997, **30**, 9 and references therein; (*c*) L. H. Gade, P. Renner, H. Memmler, F. Fecher, C. H. Galka, M. Laubender, S. Radojevic, M. McPartlin and J. W. Lauher, *Chem. Eur. J.*, 2001, **7**, 2563.
6 D. A. Evans, T. Rovis, M. C. Kozlowski, C. W. Downey and J. S. Tedrow, *J. Am. Chem. Soc.*, 2000, **122**, 9134 and references therein.
7 E. N. Jacobsen, *Acc. Chem. Res.*, 2000, **33**, 421 and references therein.
8 (*a*) R. Quinn, J. Mercer-Smith, J. N. Burstyn and J. S. Valentine, *J. Am. Chem. Soc.*, 1984, **106**, 4136; (*b*) G. E. Wuenschell, C. Tetreau, D. Lavalette and C. A. Reed, *J. Am. Chem. Soc.*, 1992, **114**, 3346; (*c*) J. P. Collman, X. Zhang, K. Wong and J. I. Brauman, *J. Am. Chem. Soc.*, 1994, **116**, 6245; (*d*) M. Momenteau and C. A. Reed, *Chem. Rev.*, 1994, **94**, 659; (*e*) C. Chang, Y. Liang, G. Avilés and S.-M. Peng, *J. Am. Chem. Soc.*, 1995, **117**, 4191; (*f*) J. E. Kickham, S. J. Loeb and S. L. Murphy, *J. Am. Chem. Soc.*, 1993, **115**, 7031; (*g*) D. M. Rudkevich, W. Verboom, Z. Brzozka, M. J. Palys, W. P. R. V. Staut-hamer, G. J. Van Hummel, S. M. Franken, S. Harkema, J. F. J. Engbersen and D. N. Reinhoudt, *J. Am. Chem. Soc.*, 1994, **116**, 4341; (*h*) N. Kitajima, H. Komatsuzaki, S. Hikichi, M. Osawa and Y. Moro-oka, *J. Am. Chem. Soc.*, 1994, **116**, 11596; (*i*) P. H. Walton and K. N. Raymond, *Inorg. Chim. Acta*, 1994, **240**, 593; (*j*) W. Yao and R. H. Crabtree, *Inorg. Chem.*, 1996, **35**, 3007; (*k*) L. M. Berreau, R. A. Allred, M. M. Makowski-Grzyska and A. M. Arif, *Chem. Commun.*, 2000, 1423; (*l*) L. M. Berreau, S. Mahapatra, J. A. Halfen, V. G. Young, Jr. and W. B. Tolman, *Inorg. Chem.*, 1996, **35**, 6339; (*m*) M. Harata, K. Jitsukawa, H. Masuda and H. Einaga, *Chem. Lett.*, 1995, 61; (*n*) A. Wada, M. Harata, K. Hasegawa, K. Jitsukawa, H. Masuda, M. Mukai, T. Kitagawa and H. Einaga, *Angew. Chem., Int. Ed.*, 1998, **37**, 798; (*o*) S. Ogo, S. Wada, Y. Watanabe, M. Iwase, A. Wada, M. Harata, K. Jitsukawa, H. Masuda and H. Einaga, *Angew. Chem., Int. Ed.*, 1998, **37**, 2102; (*p*) B. S. Hammes, V. G. Young, Jr. and A. S. Borovik, *Angew. Chem., Int. Ed.*, 1999, **38**, 666; (*q*) Z. Shirin, B. S. Hammes, V. G. Young, Jr. and A. S. Borovik, *J. Am. Chem. Soc.*, 2000, **122**, 1836; (*r*) C. E. MacBeth, A. P. Golombek,

V. G. Young, Jr., C. Yang, K. Kuczera, M. P. Hendrich and A. S. Borovik, *Science*, 2000, **289**, 938; (*s*) C.-Y. Yeh, C. J. Chang and D. G. Nocera, *J. Am. Chem. Soc.*, 2001, **123**, 1513.

9 (*a*) T. Kawamoto, O. Prakash, A. L. Rheingold, B. Ostrander and A. S. Borovik, *Inorg. Chem.*, 1995, **34**, 4294; (*b*) T. Kawamoto, B. S. Hammes, B. Haggerty, G. P. A. Yap, A. L. Rheingold and A. S. Borovik, *J. Am. Chem. Soc.*, 1996, **118**, 285; (*c*) T. Kawamoto, B. S. Hammes, R. Ostrander, A. L. Rheingold and A. S. Borovik, *Inorg. Chem.*, 1998, **37**, 3424; (*d*) Q. Yu, T. E. Baroni, L. Liable-Sands, A. L. Rheingold and A. S. Borovik, *Tetrahedron Lett.*, 1998, **39**, 6831–6834.

10 B. N. Figgis and R. S. Nyholm, *J. Chem. Soc.*, 1958, 4190.

11 The N ··· Cl(1) distances found in $[CuH_2\mathbf{1}^{Me}(Cl)\cdot Cl]^{2-}$ and $[CuH_2\mathbf{1}^{Me}(OAc)\cdot Cl]^{2-}$ are slightly longer than the reported average length of 3.181(6) Å for single N_{sp^2}–H to chloride ion interactions having N–H–Cl angles greater than 140°. (*a*) T. Steiner, *Acta Crystallogr., Sect. B*, 1998, **54**, 456; (*b*) G. Aullón, D. Bellamy, L. Brammer, E. A. Bruton and A. G. Orpen, *Chem. Commun.*, 1998, 653.

12 Representative examples: (*a*) T. J. Greenhough and M. F. C. Ladd, *Acta Crystallogr., Sect. B.*, 1977, **33**, 1266; (*b*) L. P. Battaglia, A. B. Corradi, U. Geiser, R. D. Willet, A. Motori, F. Sandrolini, L. Antolini, T. Manfredini, L. Menabue and G. C. Pellacani, *J. Chem. Soc., Dalton Trans.*, 1988, 265; (*c*) U. Geiser, R. M. Gaura, R. D. Willet and D. X. West, *Inorg. Chem.*, 1986, **25**, 4203.

13 I. Pabst, H. Fuess and J. W. Bats, *Acta Crystallogr., Sect. C*, 1987, **43**, 413.

14 A. Colombo, L. Menabue, A. Motori, G. C. Pellacani, W. Porzio, F. Sandrolini and R. D. Willett, *Inorg. Chem.*, 1983, **19**, 2900.

15 P. D. Beer, M. G. B. Drew and R. Jagessar, *J. Chem. Soc., Dalton Trans.*, 1997, 881.

16 K. Kavallieratos, S. Hwang and R. H. Crabtree, *Inorg. Chem.*, 1999, **38**, 5184.

17 For a current review on the use of ferrocenyl groups in ion sensing see: P. D. Beer, *Acc. Chem. Res.*, 1998, **31**, 71.

18 Other examples of redox-active receptors: (*a*) M. Scherer, J. L Sessler, A. Gebauer and V. Lynch, *Chem. Commun.*, 1998, 85; (*b*) M. M. G. Antonisse and D. N. Rheinhoudt, *Chem. Commun.*, 1998, 443; (*c*) P. D. Beer, F. Szemes, V. Balzani, C. M. Sala, M. G. B. Drew, S. W. Bent and M. Maestri, *J. Am. Chem. Soc.*, 1997, **119**, 11864; (*d*) J. L. Atwood, K. T. Hollman and J. W. Steed, *Chem. Commun.*, 1996, 1401.